
Objective-Agnostic Enhancement of Molecule Properties via Multi-Stage VAE

Chenghui Zhou

Department of Machine Learning
Carnegie Mellon University
chenghuz@andrew.cmu.edu

Barnabás Póczos

Department of Machine Learning
Carnegie Mellon University
bapoczos@cs.cmu.edu

Abstract

Variational autoencoder (VAE) is a popular method for drug discovery and various architectures and pipelines have been proposed to improve its performance. However, VAE approaches are known to suffer from poor manifold recovery when the data lie on a low-dimensional manifold embedded in a higher dimensional ambient space [Dai and Wipf, 2019]. The consequences of it in drug discovery are somewhat under-explored. In this paper, we explore applying a multi-stage VAE approach, that can improve manifold recovery on a synthetic dataset, to the field of drug discovery. We experimentally evaluate our multi-stage VAE approach using the ChEMBL dataset and demonstrate its ability to improve the property statistics of generated molecules substantially from pre-existing methods without incorporating property predictors into the training pipeline. We further fine-tune our models on two curated and much smaller molecule datasets that target different proteins. Our experiments show an increase in the number of active molecules generated by the multi-stage VAE in comparison to their one-stage equivalent. For each of the two tasks, our baselines include methods that use learned property predictors to incorporate target metrics directly into the training objective and we discuss complications that arise with this methodology.

1 Introduction

The use of generative models in the domain of drug discovery has recently seen rapid progress. These methods can leverage large-scale molecule archives describing the structure of existing drugs to synthesize novel molecules with similar properties as potential candidates for future drugs [Duvinaud et al., 2015, Liu et al., 2018, Segler et al., 2018, You et al., 2018, Jin et al., 2018, 2020a, Polykovskiy et al., 2020, Jin et al., 2020b, Satorras et al., 2021, Maziarz et al., 2021, Hoogeboom et al., 2022]. There are two common ways of representing the structure of molecules: Simplified Molecular Input Line Entry System (SMILES) [Weininger, 1988] and molecular graphs [Bonchev, 1991]. Graph neural networks can make effective use of the rich molecular graph representations by taking into account atoms, edges, and other structural information. SMILES strings convey less information about the molecular structure, but are more compatible with conventional sequence models (e.g., RNNs). Being able to generate valid molecules is the first step to AI-driven drug discovery and various solutions have been proposed to this problem. For example, GNN methods [Liu et al., 2018, Simonovsky and Komodakis, 2018, Jin et al., 2020a, Maziarz et al., 2021] can constrain the output space based on the chemical rules and SMILES-based approaches [Gómez-Bombarelli et al., 2018, Blaschke et al., 2018] can benefit from the abundant molecular data.

Besides structural validity, various chemical properties of the generated molecules, such as drug-likeness (QED) [Bickerton et al., 2012], Synthetic Accessibility (SA) [Ertl and Schuffenhauer, 2009] and molecular weight (MW) are critical factors when deciding whether candidate molecules can be

synthesized in a laboratory and if they can be effective in real-world applications. A molecule’s activity level on protein targets, whether to inhibit or to activate, is another very important property when treating specific diseases. A molecule that interacts successfully with the protein target is considered active and an activity score is measured based on how effective it is either to activate or inhibit the protein target’s biological function. Researchers collected large molecule datasets, such as ChEMBL [Mendez et al., 2019] and ZINC [Irwin and Shoichet, 2005], that contain an array of bioactive molecules together with information about their properties and protein targets. By training on a curated set of molecules, the generative models can learn to generate new molecules that are similar in properties to those in the training set in order to produce novel drug candidates that satisfy multiple objectives, e.g. being drug-like and active against multiple protein targets. Benchmark metrics [Polykovskiy et al., 2020, Brown et al., 2019] are created to measure how similar the generated molecules are to the target dataset structurally and property-wise. The state-of-the-art results, however, show that there is still room for improvements. Multi-objective generation by incorporating property predictors in the training pipeline [Jin et al., 2020b, Maziarz et al., 2021] is a promising avenue to address this type of problems, but there are also potential drawbacks, e.g. overfitting to the property predictor, or conflicting objectives that results in improving some objectives while degrading others.

In this paper, we introduce an objective-agnostic and easy-to-implement technique to improve existing VAE-based molecule generation models – training additional stages of VAE’s to generate latent representations for the previous-stage VAE. To show how this approach can enhance the manifold recovery of VAE models, we first study a simple MLP model trained on a synthetic sphere dataset. We then evaluate our method in an unconstrained molecule generation task and a fine-tuning task. In these experiments, we demonstrate the following claims:

- The multi-stage VAE is able to bring the property statistics of the generated molecules closer in distribution to the testing set in experiments on the ChEMBL dataset for unconstrained molecule generation;
- Fine-tuning the multi-stage VAE on the curated active molecules of two protein targets results in substantially more active outputs than fine-tuning only the first-stage model;
- In the tasks we described above, our method can achieve comparable or better results than specialized methods that directly optimize one or multiple target objectives using learned property predictors.

2 Related Work

We structure our discussing based on the type of molecular representation underlying the individual methods. Most prior approaches fall into one of the following families – namely, the SMILES string approach, the molecular graph approach and the 3D point set approach. Many approaches have been proposed to generate molecules as SMILES strings [Segler et al., 2018, Gómez-Bombarelli et al., 2018]. Kusner et al. [2017] and Dai et al. [2018] took advantage of the syntax of the SMILES strings and constrained the output of the VAE model in order to improve the validity of the generated molecules. Generative adversarial models have also been proposed to generate SMILES strings [Kadurin et al., 2017, Prykhodko et al., 2019, Guimaraes et al., 2017]. Molecular graphs carry more information about the molecular structures than the SMILES string format, and GNN can effectively incorporate the additional information into the learning process [Duvenaud et al., 2015, Liu et al., 2018, Maziarz et al., 2021]. Jin et al. [2018] proposed to generate molecular graphs in two steps – generate the tree-structured scaffolds first, and then combine these with the substructures to form molecules. Jin et al. [2020a] improved upon this prior result and proposed to generate new molecules via substructures in a coarse-to-fine manner to adapt to larger molecules, such as polymers. Satorras et al. [2021] introduced an equivariant graph neural network that can operate on molecular graphs. 3D representations of molecules are gaining traction in the research communities as they describe detailed spatial information of the molecules [Gebauer et al., 2019, 2022, Luo et al., 2021, Hoogetboom et al., 2022]. However, none of the methods use the VAE framework. The goal of our paper is to improve upon the existing VAE-based approaches. Other generative approaches to drug discovery include generative adversarial models [Kadurin et al., 2017, Prykhodko et al., 2019, Guimaraes et al., 2017] and diffusion models [Hoogetboom et al., 2022, Xu et al., 2022, Vignac et al., 2022].

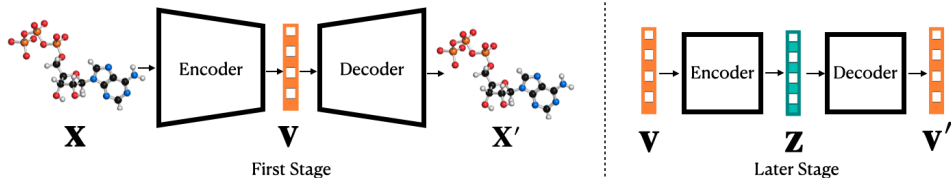


Figure 1: Overview of multi-stage VAE. In the first stage, the VAE trains on the molecule data x_i and obtains the latent variables v_i from x_i . The later-stage VAE is trained on the latent variables of the previous-stage VAE. In this figure, v_i 's become the input to the second VAE. The later-stage VAE's input dimension is equal to the output dimension. During sampling time, we sample $z \sim \mathcal{N}(0, I)$ and obtain v from the decoder. The output of a later-stage VAE decoder is used as the latent variable for the previous-stage VAE decoder until the latent variable is decoded into a molecule in the first-stage.

3 Method

The VAE framework [Kingma and Welling, 2013] has enabled great success in the image generation domain and more recently VAE-based approaches have become a popular approach for addressing the molecule generation problem. Many sophisticated architectures have been proposed to adapt the VAE approach to molecular data [Kusner et al., 2017, Dai et al., 2018, Jin et al., 2019, Satorras et al., 2021]. However, perfecting the underlying neural architecture does not remedy VAE's learning deficiency in manifold recovery [Dai and Wipf, 2019, Koehler et al., 2021]. In the case of high-dimensional data that lies on low-dimensional manifolds such as images and molecular representations, Koehler et al. [2021] found that the VAE is not guaranteed to recover the manifold where the nonlinear data lie. We show that a multi-stage VAE method can improve manifold recovery as demonstrated in a synthetic experiment (Figure 2) and can further enhance the performance of pre-existing VAE models.

3.1 Variational Autoencoder

The variational inference framework assumes that the data x is generated from a latent variable $z \sim p(z)$. The prior $p(z)$ is assumed to be a multivariate standard normal distribution in the application of a VAE. Let ϕ be the variational parameters and θ denotes the generative parameters, the VAE model consists of a tractable encoder $q_\phi(z|x)$ and a decoder $p_\theta(x|z)$. A VAE model seeks to maximize the likelihood of the data, denoted as $\log p_\theta(x) = \log \int p(z)p_\theta(x|z)dz$. However, the marginalization is intractable in practice due to the inherent complexity of the generator, or the decoder, thus an approximation of the objective is needed. The encoder and the decoder work together to approximate a lower bound to the log likelihood of the data. Ideally, by optimizing this lower bound we aim to increase the likelihood. This approximation enables the efficient posterior inference of the latent variable z given the output x_i and for marginal inference of the output variable x . The objective function of VAE consists of a KL divergence term D_{KL} and a reconstruction term:

$$\mathcal{L}(\theta, \phi; x) = -D_{KL}(q_\phi(z|x) || p(z)) + \mathbb{E}_{q_\phi(z|x)}[\log p_\theta(x|z)] \leq \log p_\theta(x) \quad (1)$$

For generation, latent representation z_i is sampled from the prior $p(z)$ which is a multivariate standard normal and the decoder transforms z_i into the output x_i .

3.2 Multi-Stage VAE

Recovery of a low-dimensional data manifold embedded in a high-dimensional ambient space is a challenging task for VAE to perform. This provides an explanation for the discrepancy in properties between the generated molecules from existing VAE approaches and the training dataset. Dai and Wipf [2019] hypothesized that training a continuous VAE with a fixed decoder variance could add additional noise to the output. While training a VAE with a tunable decoder variance, they observed that the decoder variance has a tendency to approach to zero and the diagonal entries of the encoder covariance to converge to either 0 or 1. A second VAE trained on the encoded latent variables of the VAE with close to 0 decoder variance yields crisper and more realistic images than a one-stage VAE. Their justification for such improvements on the second stage is that the first stage VAE recovers the manifold where the data lie on as the decoder variance approaches 0 and the second stage VAE recovers the density of the data. However, Koehler et al. [2021] showed that when the

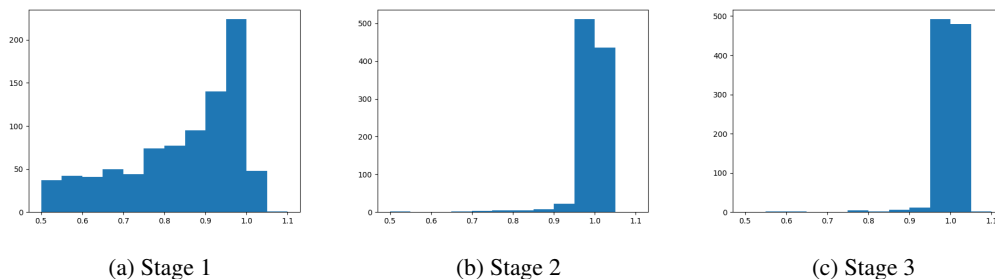


Figure 2: Multi-stage VAE on synthetic data. The x -axis represents the norm of the data point and the y -axis represents the number of data points that are of x distance away from the unit sphere center. The ground-truth data’s histogram should be a Dirac delta at location 1. The figure for stage 1 shows that most of the generated points fall *inside* of the sphere instead. The sphere surface is mostly recovered and improved starting from stage 2.

data is nonlinear, neither the manifold nor the density is guaranteed to be recovered by a one-stage VAE with tunable decoder variance. Even though this conclusion rendered the reasoning behind a 2-stage VAE invalid, the algorithm itself is not without merits. Without limiting ourselves to only 2 stages of VAE, we demonstrate in the following synthetic experiment that a multi-stage VAE can improve manifold recovery. This can also improve the properties of generated molecules as we will demonstrate in Section 4.

Synthetic Experiment We demonstrate that a multi-stage VAE setup improves the recovery of the manifold in a synthetic experiment with data generated from a ground-truth manifold (see Figure 2). We generated data from a 2-dimensional unit sphere (the norms of all the generated data points are 1). The 3-dimensional vectors are then padded with 16 dimensions of zeros to embed the data in a higher-dimensional ambient space. In this case, the intrinsic dimension of the data is 2 and the ambient dimension is 19. We trained on this data in 3 stages – meaning, the latent representations from the previous stage are used for training in the next stage. For the second and the third stage VAE, the latent dimension is set to be the same as their input (Figure 1). The decoder variance is tunable for all stages and the decoder variance of the first stage approaches 0 upon convergence. During sampling, the output of the later stage VAE becomes the latent of the previous stage VAE. The last-stage VAE’s latents are sampled from a standard normal distribution. We sample 1000 data points to visualize the results in the histograms. We observe that the VAE in the first stage *does not* recover the manifold and many of the generated data points fall *inside* of the sphere, echoing the finding by Koehler et al. [2021]. In the second and third stage, we see that more data points fall *close to* the sphere, indicating a better recovery of the manifold. The third-stage has slightly fewer points falling below the distance of 0.95 to the origin than the second.

Application on Molecule Generation The synthetic experiment is run on continuous data with a simple feed-forward architecture for both the decoder and the encoder. In this simple setting, two conditions on the first-stage VAE are satisfied for improvements in the later stage to occur [Dai and Wipf, 2019]: i) the decoder variance converges to 0; and, ii) the entries in the diagonal of the encoder variance converge to either 0 or 1. The first condition can be applied to VAE’s with multinomial setup common to molecule generation tasks and the decoder variance approaching zero is equivalent to the output being deterministic given the same latent variable. The second condition can also be verified because the latent space of the VAE models for molecule generation is generally continuous. However, the VAE architectures used for molecule generation are much more complex. Molecular data is discrete and the architectures for encoders and decoders can be hierarchical or sequential in their generation process. In Section 4, we examine how well each of the models we test on fulfills the two conditions outlined for the continuous model. We also provide empirical studies on the suitability of a multi-stage VAE approach in the molecule generation domain by thorough evaluation on the samples’ quality using structural and property statistics [Polykovskiy et al., 2020]. We find that the multi-stage VAE helps to generate molecules that are more similar in property statistics to the ones in the testing dataset. Below we present the precise steps to train a multi-stage VAE (Figure 1):

1. Train a VAE on the molecular dataset $\{x_i | i = 1, 2, \dots, n\}$, and upon convergence, save the latent variables $v_i \sim q_\phi(v|x_i)$ for all the molecules in the dataset;
2. With $\{v_i | i = 1, 2, \dots, n\}$ as input, train an additional stage of VAE with tunable decoder variance and the latent of this stage is denoted as u . We use feed-forward architectures for both the decoder $p_{\theta'}(v|u)$ and the encoder $q_{\phi'}(u|v)$. They both follow Gaussian distributions. The dimension of v is equal to u . Repeat this step to train on the $\{u_i | i = 1, 2, \dots, n\}$ in place of v_i 's until the final stage, and the last latent variable is denoted as z .
3. During the generation process, sample the latent representation of the last stage VAE, $z_i \sim \mathcal{N}(0, I)$. Obtain the output from the current stage decoder $u_i \sim p_{\theta'}(u|z)$ as the input to the previous stage decoder. Repeat until we reach the first stage VAE and get the molecule sample x_i from the first stage decoder via $x_i \sim p_\theta(x|v)$.

We observe in our experiments that, for each additional stage of VAE we train, the decoder variance converges to a larger value than the previous one (details in Appendix B). And when the new stage's decoder variance converges to 1, the improvements become minimal. One way to interpret this method is that while the first-stage VAE learns a deterministic mapping between the latent representations and the molecular output, the later-stage VAEs learn to map standard normal distribution to the distribution of the latent space of the first-stage VAE. This is because the latent variables of the first-stage VAE do not necessarily follow the standard normal distribution as is generally assumed [Dai and Wipf, 2019]. In the next section, we experiment on three pre-existing VAE models for molecule generation and verify if they meet the two conditions outlined for the continuous synthetic setting earlier. We also show that the multi-stage VAE can increase the number of active molecules generated when fine-tuning for a protein target.

4 Experiments

In this section, we demonstrate the effectiveness of our methods on two generation tasks. First, our algorithm learns to generate molecules by training on a large molecular database (i.e., ChEMBL), and we show that a multi-stage VAE is able to improve upon the one-stage VAEs in property statistics among the generated molecules. Second, our algorithm is fine-tuned on two curated molecular datasets that are active against two different protein targets (JAK2 and EGFR), and we show that the multi-stage VAE also improves the activity rate among the generated molecules.

4.1 Unconstrained Generation

We adopt three existing VAE approaches – hierarchical GNN [Jin et al., 2020a], MoLeR [Maziarz et al., 2021], and character-level RNN [Polykovskiy et al., 2020] – to compare the effects of multi-stage VAE on different model architectures. We also adopt a GAN-based model [Prykhodko et al., 2019] as an additional comparison. We conduct experiments on the ChEMBL [Mendez et al., 2019] dataset – it consists of 1,799,433 bioactive molecules with drug-like properties. It is split into training, testing, validation datasets containing 1463k, 81k, and 81k molecules respectively. Details on our evaluation metrics are in Appendix A. Below we introduce the details of the models used in this study:

Hierarchical GNN: This method first extracts chemically valid motifs, or substructures, from the molecular graph such that the union of these motifs covers the entire molecule. The model consists of a fine-to-coarse encoder that encodes from atoms to motifs and a coarse-to-fine decoder that selects motifs to create the molecule while deciding the attachment point between the motif and the emerging molecule. We use the configuration from the original model. The latent dimension of the VAE is 20 and we use 0.1 as the KL coefficient.

MoLeR GNN: Similarly to the hierarchical GNN, this method also extracts motifs in order to generate molecules piece by piece. The method's objective includes a regression term to match the true properties of the molecules and the predicted molecule properties from the latent variables. We implement our multi-stage method without such term and compare the property metrics of the generate molecules from our method to directly matching them in the training objective as "MoLeR + prop" in Table 1. We reduce the latent dimensions to 64 and use all the other original configuration.

Vanilla RNN: The inputs to the model are SMILES strings and the vocabulary consists of the low-level symbols in the SMILES strings. The encoder is a 1-layer GRU and the decoder is a 3-layer

GRU. The latent dimension of the VAE is 128. We use the original configuration except a reduced KL coefficient of 0.01.

Latent GAN: This is also a 2-stage method. The first stage is a heteroencoder that takes SMILES strings as input while the second stage is a Wasserstein GAN with gradient penalty (WGAN-GP) that trains on the latent variables of the first stage VAE. The heteroencoder consists of an encoder and a decoder like an autoencoder and is trained with categorical cross-entropy loss. Afterwards, the GAN is trained to generate latent vectors for the decoder from the heteroencoder. We use the original parameters for training.

Stage #	Sample Quality				Structural Statistics			Property Statistics			
	Valid \uparrow	Unique \uparrow	Novelty \uparrow	FCD \downarrow	SNN \uparrow	Frag \uparrow	Scaf \uparrow	LogP \downarrow	SA \downarrow	QED \downarrow	MW \downarrow
HGNN#1	1.0	1.0	0.99	5.1	0.42	0.97	0.46	0.92 _{0.016}	0.070 _{4.3e-3}	0.024 _{9.5e-4}	68.8 _{0.83}
HGNN#2	1.0	1.0	0.99	1.1	0.41	1.0	0.43	0.095 _{0.019}	0.069 _{3.8e-3}	0.0067 _{1.0e-3}	5.0 _{0.72}
HGNN#3	1.0	1.0	1.0	1.2	0.41	1.0	0.46	0.059 _{4.5e-3}	0.069 _{6.3e-3}	0.016 _{1.6e-3}	7.7 _{0.42}
MoLeR#1	1.0	1.0	0.99	2.1	0.41	0.96	0.48	0.16 _{6.78e-3}	0.028 _{1.96e-3}	0.047 _{2.78e-3}	9.6 _{0.70}
MoLeR #2	1.0	1.0	0.99	2.2	0.42	0.96	0.53	0.12 _{6.13e-3}	0.041 _{4.31e-3}	0.036 _{9.25e-4}	6.8 _{0.71}
MoLeR #3	1.0	1.0	0.99	1.8	0.42	0.96	0.49	0.087 _{6.16e-3}	0.031 _{2.81e-3}	0.028 _{2.31e-3}	8.2 _{4.0e-01}
MoLeR + prop	1.0	1.0	0.99	2.1	0.43	0.97	0.49	0.11 _{1.03e-02}	0.13 _{2.51e-03}	0.033 _{8.65e-04}	6.6 _{4.80e-01}
RNN#1	0.86	1.0	1.0	1.84	0.38	1.0	0.38	0.088 _{7.8e-3}	0.25 _{7.8e-3}	0.0088 _{1.6e-3}	3.2 _{0.55}
RNN#2	0.87	1.0	1.0	1.86	0.38	1.0	0.36	0.099 _{5.5e-3}	0.27 _{7.7e-3}	0.0099 _{1.5e-3}	2.8 _{0.29}
LatentGan	0.77	0.98	0.99	17.3	0.34	0.68	0.21	0.69 _{0.019}	0.63 _{7.3e-3}	0.04 _{7.20e-3}	27.2 _{0.88}

Table 1: Properties of the generated molecules trained on the ChEMBL dataset.

We sample 10,000 molecules from each model to generate the results in Table 1. We include sample quality, structural and property statistics. The results in the tables are averaged over 6 sets of samples generated with different random seeds from the model. We include the standard deviations for the property statistics but eliminated the rest as those are below 0.01.

The HGNN#2 improves upon the first stage by many folds on property statistics. The most notable improvement from the ChEMBL dataset is the QED (from 0.024 to 0.0067), MW (from 68.8 to 5.0) and LogP (0.92 to 0.059). A lower value on these statistics for the molecules signals that they are much more similar to the test set in these properties. Structural statistics generally did not change a lot throughout the 2-stage and 3-stage training. The performance on these metrics of the later stages models may be bottle-necked by the first-stage graph decoder. We also repeat the second-stage VAE to perform the third-stage, but there is no consistent improvement from the second stage across the board.

We trained three stages of the MoLeR model. The second stage improves upon the first stage in three (LogP, QED and MW) out of four metrics, while the third stage further improves upon the second stage in three (LogP, SA and QED) out of four metrics. Overall, MoLeR #3 improves upon MoLeR #1 in all property metrics except SA (from 0.028 to 0.031, only slightly higher). In LogP and QED, the metric goes down almost a half from 0.16 to 0.087 and from 0.047 to 0.028. The regression term in the "MoLeR + prop" optimizes over LogP, SA and MW. In two of these three metrics, "MoLeR + prop" reaches lower statistics than MoLeR#1, where such regression term is left out of the objective, but the SA metric of "MoLeR + prop" is more than four times higher than without the regression term. This highlights the challenges of directly matching multiple statistics at once during training – the objectives could be conflicting with each other and lead to unexpected results. Eventually, the MoLeR#3 reaches lower property statistics than "MoLeR + prop" in three (LogP, SA and QED) out of four metrics.

The second stage to the RNN model performs worse than the first stage in three out of four metrics. The RNN VAE’s training process does not follow a standard VAE training procedure – the SMILES strings are input to both the encoder and decoder. This allows the decoder to rely less on the latent variables during the decoding process. Our hypothesis for the poor performance of the multi-stage VAE with the RNN model as the first-stage is that the variance of the first-stage decoder did not fulfill the condition of approaching 0 upon convergence and we will discuss more on that next.

Verification on the Encoder and Decoder Variance Conditions We investigate how well each of the three first-stage models fulfill the original conditions in a continuous setting for improvements in the later stages to occur. The examination can also help explain the different behaviors from them. We present our findings in Table 2.

1. *The decoder variance of the first-stage model converges to zero.* Variance in a discrete generation setting is not easy to measure, but we can substitute variance calculation with a

simple experiment – input the same latent vector into the trained decoder for 1000 times, the number of distinct molecules the model generates can give us an indication on if the decoder variance is approaching zero. We observe that for both of the GNN models, all 1000 identical latent vectors generate 1000 identical molecules (Table 2 column "Decoder Diversity"). We can consider both models to have zero decoder variance. In contrast, the RNN model generates 1000 distinctive SMILES strings. Thus, its decoder variance did not approach 0 and our earlier hypothesis is verified.

2. *Each entry of the encoder variance diagonal either converges to 0 or 1.* We allow for 0.1 of tolerance around 0 and 1 and we find the following: The HGNN model’s 20-dimensional encoder variance diagonal has all converged to 0; RNN’s 128-dimensional encoder variance diagonal have converged to 111 of 1’s, 15 of 0’s; and MoLeR’s 64 dimensions of encoder variance diagonal have converged to 45 of 1’s, 6 of 0’s. The rest of the dimensions fall somewhere in between 0.1 and 0.9 as in Table 2’s first three columns.

Stage 1 Model	$x < 0.1$	$0.1 \leq x \leq 0.9$	$x > 0.9$	Decoder Diversity
HGNN	20	0	0	1
MoLeR	6	13	45	1
RNN	15	2	111	1000

Table 2: The first three columns document the number of encoder variance diagonal value x that fall into either of the three categories: $x < 0.1$, $0.1 \leq x \leq 0.9$ and $x > 0.9$, and the last column document the number of unique SMILES by inputting 1000 identical latent vectors.

Overall, we see that the HGNN conforms to the conditions set for the simple continuous settings and the multi-stage VAE with HGNN as first-stage is able to improve significantly on the second stage and improve slightly in certain metrics on the third. MoLeR model is able to partially fulfill the conditions and the multi-stage VAE is still able to yield better results than the first-stage. The RNN model does not fulfill any of the two conditions and the outcomes from training the multi-stage VAE with RNN as the first-stage does not follow the synthetic experiments (Figure 2) that show improvements in later stages.

4.2 Generation for a Protein Target

In addition to unconstrained generation of molecules, we also explore generating molecules that target a specific protein. We pretrain the MoLeR model and a multi-stage VAE (with MoLeR as the first-stage) on the ChEMBL dataset and fine-tune them on two curated, and much smaller, datasets [Korshunova et al., 2022] consisting of molecules that are active inhibitors of Janus Kinase 2 (JAK2) and inhibitors of the Epidermal Growth Factor (EGFR). For each of the protein target, the regression dataset contains the molecules and their corresponding activity scores (from 0 to 10). A score above 6 is considered active. The dataset size is around 19k for JAK2, in which around 15.6k are active, and around 15k for EGFR, in which around 7.8k are active. The full dataset is used to train a regressor of the activity score while only the active molecules are used to fine-tune the VAE. We divide each dataset by 80%, 10% and 10% for training, validation and testing purposes for both the VAE and the predictor. In addition, there is a separate classification dataset for each protein target – 60k for JAK2 and 50k for EGFR – containing only the binary activity information of each molecule. 10% of the dataset is used for testing the predictor.

Metrics We evaluate our method and baseline methods in three general categories: activity scores, diversity and novelty (Table 3 and 4). All evaluations are reported with means and standard deviations across 5 random seeds used to generate 5 datasets with 1000 molecules each. Particularly for activity scores, we report both the mean score and percentage of active molecules (6 as the cutoff point) in a dataset from two different regressors – a Chemprop (CPR) [Yang et al., 2019] model, and a Random Forest (RFR) model with Morgan fingerprint features [Rogers and Hahn, 2010]. Both regressors reach an RMSE of 0.5 for the JAK2 dataset and 0.6 for the EGFR dataset. In addition to the regressors, we also train two classifiers using Chemprop (CPC) and Random Forest (RFC) with Morgan fingerprint features on the classification dataset. All predictors’ performances on the active test set split are included in Table 3 and 4 as a reference. Novelty is defined as the fraction of molecules with its nearest neighbor similarity in the active training set lower than 0.4. Diversity is calculated based on the pairwise molecular distance $\text{sim}(X, Y)$ within the generated dataset. The

function $\text{sim}(\cdot, \cdot)$ is defined as the Tanimoto distance over Morgan fingerprints of two molecules. We define the two metrics as follows [Jin et al., 2020b]:

$$\text{Diversity} = 1 - \frac{2}{n(n-1)} \sum_{X,Y} \text{sim}(X, Y) \quad \text{Novelty} = \frac{1}{n} \sum_{\mathcal{G}} \mathbf{1}[\text{sim}(\mathcal{G}, \mathcal{G}_{S,N,N}) < \mathbf{0.4}] \quad (2)$$

Methods We compare the generated molecules from the fine-tuned multi-stage VAE to the fine-tuned MoLeR model. In addition, we include RationaleRL [Jin et al., 2020b] as an additional reinforcement learning-based baseline. We obtained the multi-stage VAE (3-stage in this case) from training on the full ChEMBL dataset as described in Section 3.2. The first-stage VAE was fine-tuned on the curated active molecules dataset after pretraining on the full ChEMBL dataset. The second and third-stage VAEs are initialized with the parameters from the corresponding stage of the pre-trained multi-stage VAE and fine-tuned on the encoded latent variables of the curated dataset from the fine-tuned previous-stage VAE. We fine-tuned the later-stage VAE’s in three ways: fine-tuning the entire model, fine-tuning only the two inner-layers connecting to the latent sampling layer, and fine-tuning only the two outer-layers connecting to the input and output. We compare the distribution of the activity scores for EGFR as predicted by the Chemprop model from the three types of fine-tuning methods and baselines in Figure 3. The quantitative metrics are shown in Table 3 and 4. Each evaluation reports metrics for the active test set as a reference.

Model Type	Activity (CPC)	Activity (CPR)	Mean (CPR)	Activity (RFC)	Activity (RFR)	Mean (RFR)	Diversity	Novelty(0.4)	Time ¹
Active Test set	0.93	0.92	7.4	0.98	0.89	7.1	0.85	0.016	-
MoLeR	0.44118e-02	0.57121e-02	6.3294e-02	0.41114e-02	0.60146e-02	6.3216e-02	0.87226e-03	0.63181e-02	4 min
RationaleRL	0.79794e-03	0.84145e-02	6.8136e-02	0.88123e-02	0.94450e-03	6.7142e-02	0.79138e-03	0.05524e-03	4.5 d
Whole-Model	0.53643e-03	0.63665e-03	6.4318e-02	0.50138e-02	0.69431e-03	6.5191e-02	0.85995e-04	0.54965e-03	1.5 h
Inner-Layer	0.79161e-02	0.87131e-02	7.4392e-02	0.88127e-02	0.90840e-03	7.0204e-02	0.71441e-03	0.17203e-02	1.25 h
Outer-Layer	0.85130e-02	0.89531e-03	7.2317e-02	0.86175e-02	0.89117e-02	6.9261e-02	0.71530e-03	0.22878e-03	1.5 h

Table 3: Evaluation of the generated molecules targeting EGFR by three fine-tuning methods: fine-tuning the whole model, fine-tuning only the inner-layers and fine-tuning the outer-layers. They are compared against baseline models such as fine-tuned MoLeR and RationaleRL. The evaluation metrics include percentage of active molecules, mean activity scores, diversity and novelty.

Model Type	Activity (CPC)	Activity (CPR)	Mean (CPR)	Activity (RFC)	Activity (RFR)	Mean (RFR)	Diversity	Novelty(0.4)	Time ¹
Active Test set	0.97	0.97	7.5	0.99	0.98	7.4	0.88	0.016	-
MoLeR	0.52115e-02	0.74689e-03	6.5117e-02	0.44173e-02	0.89124e-02	6.7244e-02	0.90562e-04	0.85671e-03	7 min
RationaleRL	0.85896e-03	0.79167e-02	6.6293e-02	0.92493e-03	0.96726e-03	6.8167e-02	0.87258e-03	0.24742e-03	8.5 d
Whole-Model	0.54831e-03	0.78102e-02	6.6222e-02	0.46113e-02	0.91590e-03	6.7116e-02	0.89447e-04	0.82780e-03	2.8 h
Inner-Layer	0.66758e-03	0.88111e-02	6.9101e-02	0.56688e-03	0.94228e-03	6.8136e-02	0.88839e-04	0.78629e-03	2.8 h
Outer-Layer	0.62277e-02	0.89837e-03	6.9372e-02	0.65123e-02	0.95196e-03	6.9153e-02	0.86129e-03	0.69537e-03	2.8 h

Table 4: Evaluation of the generated molecules targeting JAK2 by three fine-tuning methods: fine-tuning the whole model, fine-tuning only the inner-layers and fine-tuning the outer-layers. They are compared against baseline models such as fine-tuned MoLeR and RationaleRL. The evaluation metrics include percentage of active molecules, mean activity scores, diversity and novelty.

For both of the protein targets, fine-tuning the multi-stage VAE in either of the three ways produces more active molecules of the protein targets than fine-tuning only the first-stage VAE (Table 3 and 4) with all predictors considered. The improvement is especially pronounced on the EGFR dataset, which is about half of the JAK2 dataset size. Particularly, fine-tuning only the inner-layers or outer-layers produces more active molecules than fine-tuning the whole model. Their activity score distribution is also more similar to the test set’s. The peak of the activity score distribution around 7 is well-captured by the two fine-tuning methods of the VAE in Figure 3a and 3b.

RationaleRL model is initialized with a generative model trained on the ChEMBL dataset and then fine-tuned with an RL algorithm. The Random-Forest classifier with Morgan fingerprint features is used as its reward signal [Jin et al., 2020b] in the fine-tuning process. RationaleRL generally has higher percentage of active molecules when predicted by the two Random Forest models than Chemprop, a sign of possible overfitting. No such pattern is observed for our methods that did not involve property predictors in the fine-tuning process. On the EGFR dataset, RationaleRL reaches higher level of activity than fine-tuned multi-stage VAE as predicted by Random Forest models but lower level of activity when predicted by Chemprop. On the JAK2 dataset, our methods have lower activity level than RationaleRL as predicted by both classifiers but both regressors have predicted similar or slightly higher activity levels on the generated molecules from our methods. Fine-tuned

¹Training on a single "NVIDIA GeForce RTX 2080 Ti" GPU.

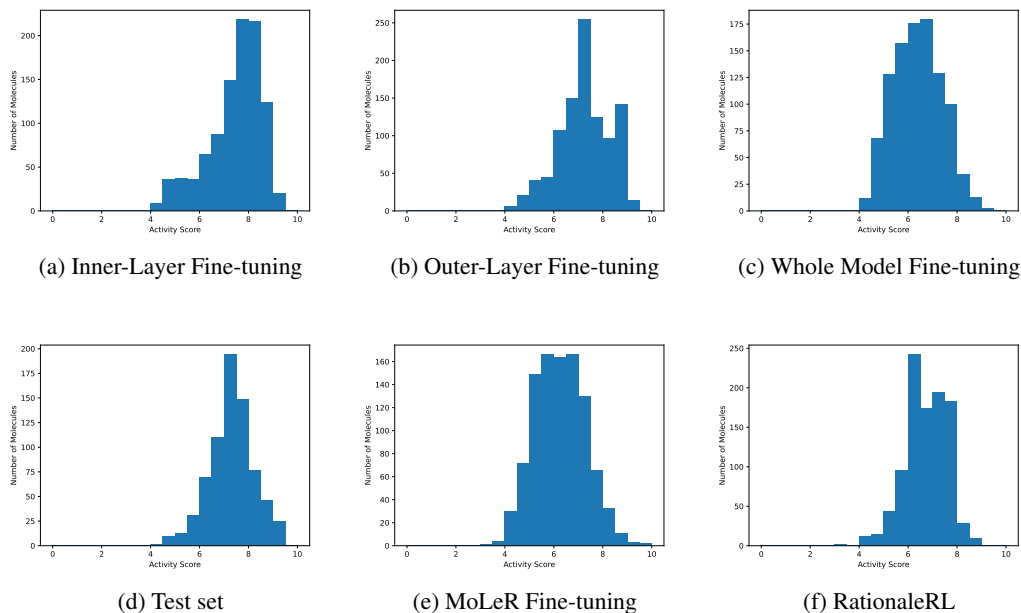


Figure 3: The distributions of the generated molecules’ activity scores on the EGFR protein predicted by the Chemprop model. We include 5 sets of molecules generated by different methods as well as the ground-truth test set. Additional activity score histograms can be found in Appendix D

multi-stage VAE is similar to RationaleRL on diversity but higher on novelty metric. Our method reaches slightly higher mean activity scores than RationaleRL on both datasets predicted by both regressors. In addition, RationaleRL is much more computationally intensive to train.

Multiple factors could contribute to the large discrepancy between regressors and classifiers’ predictions on the dataset generated by our method for JAK2. It could be that the classifiers are more adept at identifying negative samples due to the larger training set, which also includes more negative examples. Another reason could be that the predictors fail to generalize to an out-of-distribution dataset, such as the generated one, despite performing well on the ground-truth data. These differing results also highlight the challenges in drawing conclusions based on property predictors, which further complicates the optimization process.

5 Discussion

In this paper, we present a novel multi-stage VAE model that enhances the properties of the generated molecules from pre-existing VAE models. It achieves the goal in an objective-agnostic way, meaning, our method does not optimize over any particular property objectives during training. Yet, it is able to achieve comparable, and sometimes better outcomes than specialized approaches that directly optimizes over one or multiple property objectives with the help of property predictors. We demonstrate this in two experiments: 1) an unconstrained generation experiment trained on ChEMBL dataset in which we compare against MoLeR [Maziarz et al., 2021] that includes regression terms in the VAE objective to match the true property values of the molecules with the predicted properties from the latent variables of the molecules; and 2) a generation for protein target experiment where our multi-stage VAE is fine-tuned on two active molecule datasets against two protein targets. We compare our method to RationaleRL [Jin et al., 2020b], which uses an activity predictor as the reward function. Our findings also bring up the complications in using property predictors for multi-objective generation, e.g. overfitting, conflicting objectives, and differing prediction results from different predictors. Addressing these issues is an important direction for future research.

References

- Guy W Bemis and Mark A Murcko. The properties of known drugs. 1. molecular frameworks. *Journal of medicinal chemistry*, 39(15):2887–2893, 1996.
- G Richard Bickerton, Gaia V Paolini, Jérémy Besnard, Sorel Muresan, and Andrew L Hopkins. Quantifying the chemical beauty of drugs. *Nature chemistry*, 4(2):90–98, 2012.
- Thomas Blaschke, Marcus Olivecrona, Ola Engkvist, Jürgen Bajorath, and Hongming Chen. Application of generative autoencoder in de novo molecular design. *Molecular informatics*, 37(1-2): 1700123, 2018.
- Danaïl Bonchev. *Chemical graph theory: introduction and fundamentals*, volume 1. CRC Press, 1991.
- Nathan Brown, Marco Fiscato, Marwin HS Segler, and Alain C Vaucher. Guacamol: benchmarking models for de novo molecular design. *Journal of chemical information and modeling*, 59(3): 1096–1108, 2019.
- Bin Dai and David Wipf. Diagnosing and enhancing vae models. *arXiv preprint arXiv:1903.05789*, 2019.
- Hanjun Dai, Yingtao Tian, Bo Dai, Steven Skiena, and Le Song. Syntax-directed variational autoencoder for structured data. *arXiv preprint arXiv:1802.08786*, 2018.
- Jörg Degen, Christof Wegscheid-Gerlach, Andrea Zaliani, and Matthias Rarey. On the art of compiling and using ‘drug-like’ chemical fragment spaces. *ChemMedChem: Chemistry Enabling Drug Discovery*, 3(10):1503–1507, 2008.
- David Duvenaud, Dougal Maclaurin, Jorge Aguilera-Iparraguirre, Rafael Gómez-Bombarelli, Timothy Hirzel, Alán Aspuru-Guzik, and Ryan P Adams. Convolutional networks on graphs for learning molecular fingerprints. *arXiv preprint arXiv:1509.09292*, 2015.
- Peter Ertl and Ansgar Schuffenhauer. Estimation of synthetic accessibility score of drug-like molecules based on molecular complexity and fragment contributions. *Journal of cheminformatics*, 1(1):1–11, 2009.
- Niklas Gebauer, Michael Gastegger, and Kristof Schütt. Symmetry-adapted generation of 3d point sets for the targeted discovery of molecules. *Advances in neural information processing systems*, 32, 2019.
- Niklas WA Gebauer, Michael Gastegger, Stefaan SP Hessmann, Klaus-Robert Müller, and Kristof T Schütt. Inverse design of 3d molecular structures with conditional generative neural networks. *Nature communications*, 13(1):1–11, 2022.
- Rafael Gómez-Bombarelli, Jennifer N Wei, David Duvenaud, José Miguel Hernández-Lobato, Benjamín Sánchez-Lengeling, Dennis Sheberla, Jorge Aguilera-Iparraguirre, Timothy D Hirzel, Ryan P Adams, and Alán Aspuru-Guzik. Automatic chemical design using a data-driven continuous representation of molecules. *ACS central science*, 4(2):268–276, 2018.
- Gabriel Lima Guimaraes, Benjamin Sanchez-Lengeling, Carlos Outeiral, Pedro Luis Cunha Farias, and Alán Aspuru-Guzik. Objective-reinforced generative adversarial networks (organ) for sequence generation models. *arXiv preprint arXiv:1705.10843*, 2017.
- Emiel Hoogetboom, Victor Garcia Satorras, Clement Vignac, and Max Welling. Equivariant diffusion for molecule generation in 3d. In *International Conference on Machine Learning*, pages 8867–8887. PMLR, 2022.
- John J Irwin and Brian K Shoichet. Zinc- a free database of commercially available compounds for virtual screening. *Journal of chemical information and modeling*, 45(1):177–182, 2005.
- Wengong Jin, Regina Barzilay, and Tommi Jaakkola. Junction tree variational autoencoder for molecular graph generation. In *International conference on machine learning*, pages 2323–2332. PMLR, 2018.

- Wengong Jin, Regina Barzilay, and Tommi Jaakkola. Hierarchical graph-to-graph translation for molecules. *arXiv preprint arXiv:1907.11223*, 2019.
- Wengong Jin, Regina Barzilay, and Tommi Jaakkola. Hierarchical generation of molecular graphs using structural motifs. In *International Conference on Machine Learning*, pages 4839–4848. PMLR, 2020a.
- Wengong Jin, Regina Barzilay, and Tommi Jaakkola. Multi-objective molecule generation using interpretable substructures. In *International conference on machine learning*, pages 4849–4859. PMLR, 2020b.
- Artur Kadurin, Sergey Nikolenko, Kuzma Khrabrov, Alex Aliper, and Alex Zhavoronkov. drugan: an advanced generative adversarial autoencoder model for de novo generation of new molecules with desired molecular properties in silico. *Molecular pharmaceutics*, 14(9):3098–3104, 2017.
- Diederik P Kingma and Max Welling. Auto-encoding variational bayes. *arXiv preprint arXiv:1312.6114*, 2013.
- Frederic Koehler, Viraj Mehta, Andrej Risteski, and Chenghui Zhou. Variational autoencoders in the presence of low-dimensional data: landscape and implicit bias. *arXiv preprint arXiv:2112.06868*, 2021.
- Maria Korshunova, Niles Huang, Stephen Capuzzi, Dmytro S Radchenko, Olena Savych, Yuriy S Moroz, Carrow I Wells, Timothy M Willson, Alexander Tropsha, and Olexandr Isayev. Generative and reinforcement learning approaches for the automated de novo design of bioactive compounds. *Communications Chemistry*, 5(1):129, 2022.
- Matt J Kusner, Brooks Paige, and José Miguel Hernández-Lobato. Grammar variational autoencoder. In *International conference on machine learning*, pages 1945–1954. PMLR, 2017.
- Qi Liu, Miltiadis Allamanis, Marc Brockschmidt, and Alexander L Gaunt. Constrained graph variational autoencoders for molecule design. *arXiv preprint arXiv:1805.09076*, 2018.
- Shitong Luo, Jiaqi Guan, Jianzhu Ma, and Jian Peng. A 3d generative model for structure-based drug design. *Advances in Neural Information Processing Systems*, 34:6229–6239, 2021.
- Krzysztof Maziarz, Henry Jackson-Flux, Pashmina Cameron, Finton Sirockin, Nadine Schneider, Nikolaus Stiefl, Marwin Segler, and Marc Brockschmidt. Learning to extend molecular scaffolds with structural motifs. *arXiv preprint arXiv:2103.03864*, 2021.
- David Mendez, Anna Gaulton, A Patrícia Bento, Jon Chambers, Marleen De Veij, Eloy Félix, María Paula Magariños, Juan F Mosquera, Prudence Mutowo, Michał Nowotka, et al. ChEMBL: towards direct deposition of bioassay data. *Nucleic acids research*, 47(D1):D930–D940, 2019.
- Daniil Polykovskiy, Alexander Zhebrak, Benjamin Sanchez-Lengeling, Sergey Golovanov, Oktai Tatanov, Stanislav Belyaev, Rauf Kurbanov, Aleksey Artamonov, Vladimir Aladinskiy, Mark Veselov, et al. Molecular sets (moses): a benchmarking platform for molecular generation models. *Frontiers in pharmacology*, 11:1931, 2020.
- Kristina Preuer, Philipp Renz, Thomas Unterthiner, Sepp Hochreiter, and Gunter Klambauer. Fréchet chemnet distance: a metric for generative models for molecules in drug discovery. *Journal of chemical information and modeling*, 58(9):1736–1741, 2018.
- Oleksii Prykhodko, Simon Viet Johansson, Panagiotis-Christos Kotsias, Josep Arús-Pous, Esben Jannik Bjerrum, Ola Engkvist, and Hongming Chen. A de novo molecular generation method using latent vector based generative adversarial network. *Journal of Cheminformatics*, 11(1):1–13, 2019.
- David Rogers and Mathew Hahn. Extended-connectivity fingerprints. *Journal of chemical information and modeling*, 50(5):742–754, 2010.
- Victor Garcia Satorras, Emiel Hoogetboom, Fabian B Fuchs, Ingmar Posner, and Max Welling. E(n) equivariant normalizing flows. *arXiv preprint arXiv:2105.09016*, 2021.

- Marwin HS Segler, Thierry Kogej, Christian Tyrchan, and Mark P Waller. Generating focused molecule libraries for drug discovery with recurrent neural networks. *ACS central science*, 4(1): 120–131, 2018.
- Martin Simonovsky and Nikos Komodakis. Graphvae: Towards generation of small graphs using variational autoencoders. In *International conference on artificial neural networks*, pages 412–422. Springer, 2018.
- Peter C St. John, Caleb Phillips, Travis W Kemper, A Nolan Wilson, Yanfei Guan, Michael F Crowley, Mark R Nimlos, and Ross E Larsen. Message-passing neural networks for high-throughput polymer screening. *The Journal of chemical physics*, 150(23):234111, 2019.
- Clement Vignac, Igor Krawczuk, Antoine Siraudin, Bohan Wang, Volkan Cevher, and Pascal Frossard. Digress: Discrete denoising diffusion for graph generation. *arXiv preprint arXiv:2209.14734*, 2022.
- David Weininger. Smiles, a chemical language and information system. 1. introduction to methodology and encoding rules. *Journal of chemical information and computer sciences*, 28(1):31–36, 1988.
- Scott A Wildman and Gordon M Crippen. Prediction of physicochemical parameters by atomic contributions. *Journal of chemical information and computer sciences*, 39(5):868–873, 1999.
- Minkai Xu, Lantao Yu, Yang Song, Chence Shi, Stefano Ermon, and Jian Tang. Geodiff: A geometric diffusion model for molecular conformation generation. *arXiv preprint arXiv:2203.02923*, 2022.
- Kevin Yang, Kyle Swanson, Wengong Jin, Connor Coley, Philipp Eiden, Hua Gao, Angel Guzman-Perez, Timothy Hopper, Brian Kelley, Miriam Mathea, et al. Analyzing learned molecular representations for property prediction. *Journal of chemical information and modeling*, 59(8):3370–3388, 2019.
- Jiaxuan You, Bowen Liu, Rex Ying, Vijay Pande, and Jure Leskovec. Graph convolutional policy network for goal-directed molecular graph generation. *arXiv preprint arXiv:1806.02473*, 2018.

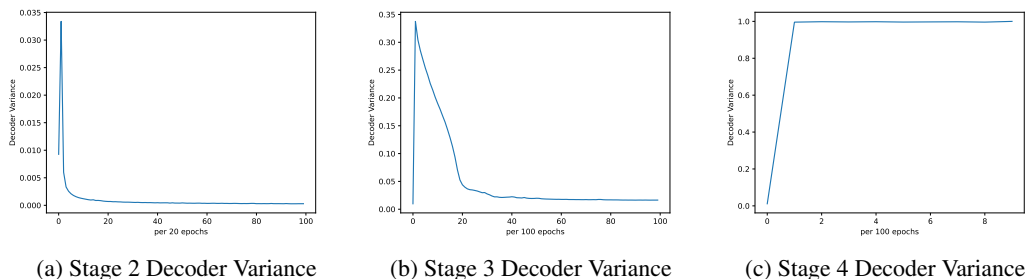


Figure 4: The decoder variance’s change over the course of training time.

A Benchmark Metrics

Property Statistics include LogP (The Octanol-Water Partition Coefficient), SA (Synthetic Accessibility Score), QED (Quantitative Estimation of Drug-Likeness) and MW (Molecular Weight). These metrics determine the practicality of the generated molecules, for example, LogP measures the solubility of the molecules in water or an organic solvent [Wildman and Crippen, 1999], SA estimates how easily the molecules can be synthesized based on molecule structures [Ertl and Schuffenhauer, 2009], QED estimates how likely it can be a viable candidate of drugs [Bickerton et al., 2012]. The values listed in the table for each metric are the Wasserstein distances between the distributions of the property statistics in the test set and the generate molecule set.

Structural statistics include SNN (Similarity to Nearest Neighbor), Frag (Fragment Similarity), and Scaf (Scaffold Similarity). These statistics calculate two molecular datasets’ structural similarity based on their extended-connectivity fingerprints [Rogers and Hahn, 2010], BRICS fragments [Degen et al., 2008] and Bemis–Murcko scaffolds [Bemis and Murcko, 1996].

The sample quality metrics are a lot more intuitive. Valid calculates the percentage of valid molecule outputs. Unique calculates the percentage of unique molecules in the first k molecules where $k = 1000$ for the ChEMBL dataset. Novelty calculates the percentage of molecules generated that are not present in the training set. FCD is the Fréchet ChemNet Distance [Preuer et al., 2018].

B Converged Decoder Variance in Different Stages

For HGNN model, the stage #2 model’s decoder variance converges to 0.067 and the stage #3 decoder variance converges to 1.0. For the RNN-VAE model, the stage #2 model’s decoder variance converges to 1.

For the MoLeR model, the stage #2 model’s decoder variance converges to 0.00013, and the stage #3 model’s decoder variance converges to 0.016. We train a stage #4 VAE and it converges to 1.0. We include the plots of the decoder variance during training at each stage in Figure 4. For both stage #2 and #3, the decoder variance briefly goes up in the beginning of the training before converges to a value much smaller. In stage #4, the decoder variance reaches 1 very quickly and the value stays unchanged. We include the results generated by a 4-stage VAE in Table 5’s #4 row.

MoLeR + prop	Sample Quality			Structural Statistics			Property Statistics				
	Valid \uparrow	Unique \uparrow	Novelty \uparrow	FCD \downarrow	SNN \uparrow	Frag \uparrow	Scaf \uparrow	LogP \downarrow	SA \downarrow	QED \downarrow	MW \downarrow
#1	1.0	1.0	0.99	2.1	0.41	0.96	0.48	0.166.78e-3	0.028 1.96e-3	0.0472.78e-3	9.60.70
#2	1.0	1.0	0.99	2.2	0.42	0.96	0.53	0.126.13e-3	0.0414.31e-3	0.0369.25e-4	6.80.71
#3	1.0	1.0	0.99	1.8	0.42	0.96	0.49	0.0876.16e-03	0.0312.81e-03	0.028 2.31e-03	8.24.0e-01
#4	1.0	1.0	0.99	1.9	0.42	0.96	0.48	0.066 7.39e-03	0.0303.27e-03	0.0291.52e-03	10.6.44e-01

Table 5: Properties of the generated molecules from the 4th-stage VAE trained on the ChEMBL dataset using MoLeR without property matching as the first stage.

C Additional Multi-stage VAE Results

In this section, we include additional results on multi-stage VAE. We train a multi-stage VAE on a polymer dataset [St. John et al., 2019] with HGNN as the first-stage. The first-stage result is included in the HGNN paper [Jin et al., 2020a]. We present the results from the second and third-stage VAE in relation to the first-stage in Table 6. We also trained two additional stages for MoLeR model with property matching included in the objective function in Table 7.

The Polymer Dataset[St. John et al., 2019] contains 86,353 polymers and it’s divided into training, test and validation set that contains 76,353, 5000 and 5000 molecules each. Polymers generally have heavier weight than the molecules in the ChEMBL dataset and the dataset size is smaller. Uniqueness is selected to be at top $k = 500$ for the polymer dataset.

HGNN	Sample Quality				Structural Statistics			Property Statistics			
	Valid \uparrow	Unique \uparrow	Novelty \uparrow	FCD \downarrow	SNN \uparrow	Frag \uparrow	Scaf \uparrow	LogP \downarrow	SA \downarrow	QED \downarrow	MW \downarrow
#1	1.0	1.0	0.57	0.62	0.67	0.98	0.37	1.3 _{0.030}	0.089 _{3.0e-3}	0.020 _{1.2e-3}	72.2 _{1.42}
#2	1.0	1.0	0.51	0.27	0.69	0.99	0.37	0.10 _{0.033}	0.031 _{3.3e-3}	0.004 _{19.5e-4}	7.7 _{1.1}
#3	1.0	1.0	0.52	0.29	0.69	0.99	0.38	0.24 _{0.017}	0.024 _{4.1e-3}	0.0024 _{2.9e-4}	9.4 _{2.3}

Table 6: Properties of the generated molecules trained on the polymers dataset.

On the polymer dataset, the second stage VAE improves significantly across all metrics – from 72.2 to 7.7 on MW, 0.020 to 0.0024 on QED, 0.089 to 0.031 on SA and 1.3 to 0.1 on LogP. In the third stage, 2 of the metrics (SA and QED) improved while the other 2 degraded.

We train a multi-stage VAE on MoLeR with property matching as the first stage. Due to the modification to the objective function, none of the analysis described in the main paper necessarily apply here, but it is still interesting to see the results.

MoLeR + prop	Sample Quality				Structural Statistics			Property Statistics			
	Valid \uparrow	Unique \uparrow	Novelty \uparrow	FCD \downarrow	SNN \uparrow	Frag \uparrow	Scaf \uparrow	LogP \downarrow	SA \downarrow	QED \downarrow	MW \downarrow
#1	1.0	1.0	0.99	2.1	0.43	0.97	0.49	0.11 _{1.03e-02}	0.13 _{2.51e-03}	0.033 _{8.65e-04}	6.6 _{4.80e-01}
#2	1.0	1.0	0.99	2.2	0.42	0.97	0.48	0.080 _{1.37-02}	0.090 _{6.03-03}	0.030 _{1.80-03}	6.0 _{2.94-01}
#3	1.0	1.0	0.99	2.0	0.43	0.97	0.41	0.096 _{1.21-02}	0.13 _{5.17-03}	0.022 _{1.68-03}	9.1 _{7.34-01}

Table 7: Properties of the generated molecules from the multi-stage VAE trained on the ChEMBL dataset using MoLeR with property matching as the first stage.

In Table 7, we see that the second-stage VAE is able to improve upon the first-stage on all metrics while the third-stage improves only upon QED while the other 3 properties degraded.

D Additional Activity Score Distribution Figures

In the main paper, we include the activity score distribution of the generated molecules trained on the EGFR dataset by Chemprop. We include the additional 3 figures that show the distribution of the activity scores generated by models trained on EGFR (Figure 6) and JAK2 dataset as predicted by Random Forest and JAK2 (Figure 7) dataset as predicted by Chemprop in Figure 5.

E Training details on multi-stage VAE

Each stage of the multi-stage VAE with HGNN as the first stage has three fully-connected layers of size 512 for both encoders and decoders in addition to the input and output layer which are of size 20 (latent dimensions). The initial decoder variance is set at 0.05. Learning rate is set at 0.0001.

Each stage of the multi-stage VAE with MoLeR as the first stage has five fully-connected layers of size 1025 for both encoders and decoders in addition to the input and output layer which are of size 64 (latent dimensions). The initial decoder variance is set at 0.007. Learning rate is set at 0.0001. We trained our model for 10000 epochs but fewer epochs (e.g. 5000) can probably achieve similar results. For fine-tuning, the decoder variance is held as constant during the process. Fine-tuning either inner-layer or extra-layer is done by loading the pre-trained model and add two extra layers either connecting to the latent layer or the output. The two extra layers are randomly initialized. The pre-trained part of the model is frozen while only the additional layers are being trained. Fine-tuning the whole model means to load the pre-trained model and only freeze the decoder variance while

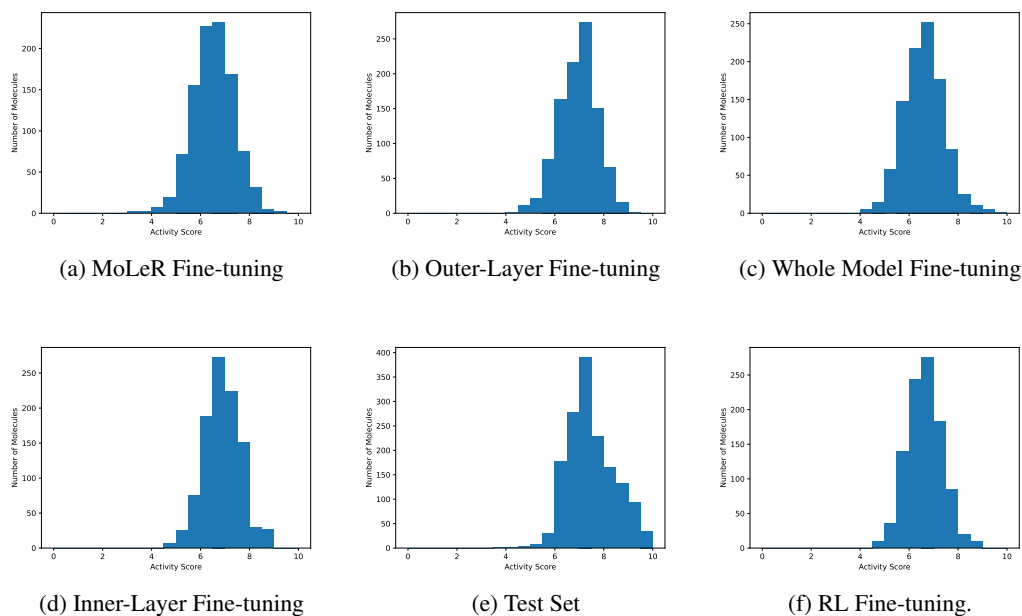


Figure 5: The distributions of the generated molecules' activity scores by the Chemprop model on the JAK2 protein in six histograms.

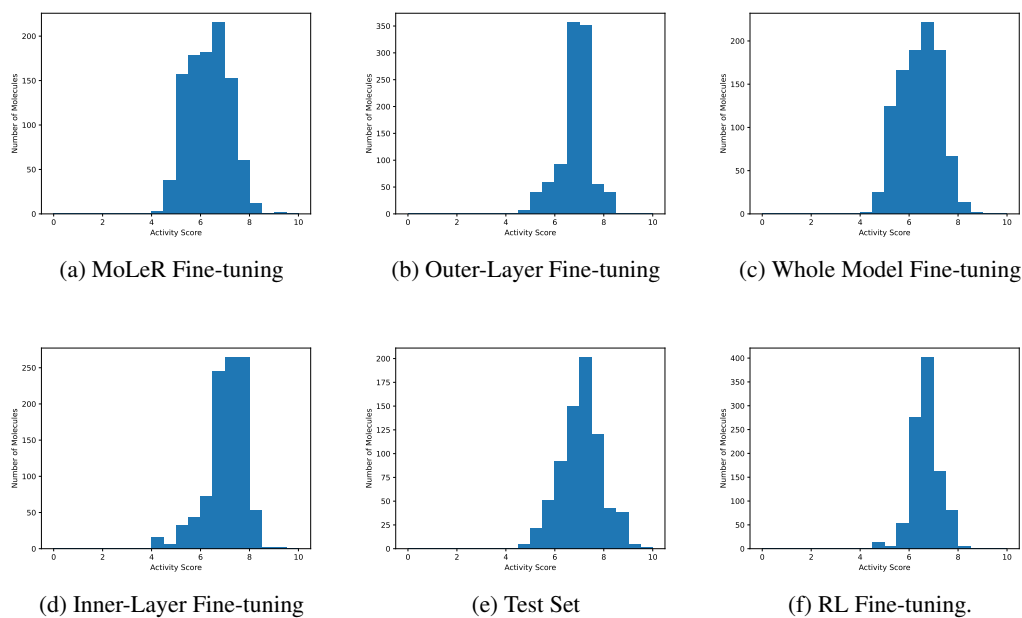


Figure 6: The distributions of the generated molecules' activity scores by the Random Forest model on the EGFR protein in six histograms.

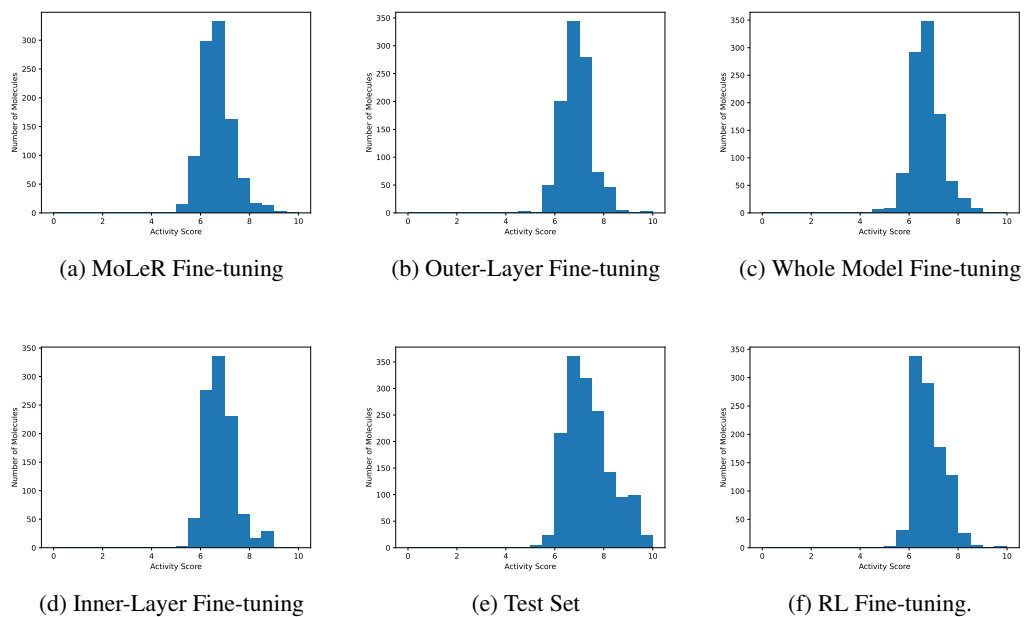


Figure 7: The distributions of the generated molecules' activity scores by the Random Forest model on the JAK2 protein in six histograms.

training the rest of it without additional layers. During fine-tuning, we use 0.0001 as the learning rate and train for 50000 epochs.